Structure and dynamics of CaO films: A computational study of an effect of external static electric field

Mikhail S. Kuklin,[1] Andrey S. Bazhenov,[2] Karoliina Honkala,[2] Sergio Tosoni,[3] Gianfranco Pacchioni,[3] and Hannu Häkkinen[1,2,*]

[1]*Department of Physics, Nanoscience Center, University of Jyväskylä, FI-40014 Jyväskylä, Finland*

[2]*Department of Chemistry, Nanoscience Center, University of Jyväskylä, FI-40014 Jyväskylä, Finland*

[3]*Dipartimento di Scienza dei Materiali, Università di Milano-Bicocca, via Cozzi 55, 20125 Milano, Italy*

(Received 2 February 2017; published 17 April 2017)

Oxide films play a significant role in a wide range of industrial fields, mostly due to the thickness-dependent variation of their properties. Recently, it has been proposed based on the experimental study that carrier transport in CaO films proceeds via strong phonon excitations with a variable signal depending on the film thickness. In this paper, we report a detailed investigation in the frame of the density functional theory of structural and electronic properties of freestanding and Mo(100)-supported CaO films, as well as phonons therein, as functions of the film thickness and intensity of the external static electric field. Our calculations demonstrate that phonon frequencies negligibly depend on the external electric field. A small gradual increase of the energy of CaO phonons upon increase of the film thickness was found to be in line with earlier experimental findings. The effect of Mo support was observed in the systematic decrease of the energy of phonons. The applied electric field showed a minor effect on the structure of CaO films, whereas electronic properties of the oxide were significantly affected. In particular, the band gap of CaO films was found to gradually decrease with the growing intensity of the external electric field, while the effect is a more pronounced for thicker films. Overall, our paper provides innovative insights into the mechanism of electron transport and electronic properties of CaO films that might lead to new potential applications of oxide materials.

DOI: 10.1103/PhysRevB.95.165423

I. INTRODUCTION

Oxide films play a fundamental role in a broad range of economically relevant fields: heterogeneous catalysis, microelectronics, optoelectronics, spintronics, corrosion protection, solar energy materials, tunneling magnetoresonance sensors, etc. [1–5]. One of the most prominent uses of oxide films is based on electron transfer [1]. The thickness of oxide film, in this sense, is a decisive factor in the mechanism of electron transport; a thin film typically proceeds with spontaneous electron tunneling and a thick film proceeds with ballistic transport, where phonons can take part. The probability of electron tunneling is decreased with growing film thickness: an electron cannot directly tunnel through thick films [4]. Beyond, typically, a 10 monolayer (ML) thickness hopping mechanism takes place and the bulk behavior is recovered. This finding represents a unique feature of oxides, and in general, of other insulating materials, that allows modification of their properties by changing film thickness; oxides at the nanoscale typically exhibit different behavior than that of bulk material [6]. Thin NaCl films, for instance, were shown to display radically different properties from those of bulk NaCl concerning electron localization and segregation [7]. Phonons, as collective excitations of the crystal lattice, play a significant role in electron transport and thermal effects in solids [8]. For example, the large width of gap states induced by Cl vacancies in NaCl thin films was explained by phonon excitations via inelastic electrons [9,10]. The longitudinal optical (LO) excitations were identified in ZnO upon charging or discharging of individual donors with the scanning tunneling microscope (STM) tip [11]. Interestingly, the phonons for FeO films supported on Pt(111) were shown to strongly depend on the film thickness, with a two-dimensional to three-dimensional transition reported starting from 3 ML [12].

Insulating calcium oxide (CaO) represents a rock salt structure in the bulk phase. This group 2 alkali earth metal oxide brings high potential due to the following aspects: (1) easy production from minerals or salts widely distributed in nature [13], (2) a good insulator due to the wide band gap, (3) active in chemical interactions due to the high basicity, (4) a good electron donor due to the low Madelung potential, and (5) delocalized electronic structure that makes easier for adsorbates to interact with the surface of oxide.

Recently, it has been proposed based on a low-temperature STM experiments that carrier transport in Mo supported CaO thin film is accompanied by strong phonon excitations [14]. Interestingly, phonon excitations showed various oscillating signals in the differential conductance (dI/dV) depending on the thickness of CaO film. Preliminary calculations in the frame of the density functional theory (DFT) revealed the correlation between the energy peak spacing of the dI/dV maxima, which is presumably due to the phonon excitations, and the Γ point LO phonon frequency of CaO films [14]. Therefore, the calculated Γ point LO phonon frequency may explain the different energy spacing of the dI/dV maxima for CaO films with different thicknesses and provide insights into the mechanism of carrier transport. The LO phonons participate in efficient coupling of moving carriers, because their symmetry makes them sensitive to local modulations in the lattice polarization. Therefore, the LO phonon might be involved in electron hopping through the CaO lattice. Despite this finding, the nature of the thickness-dependent oscillating signals in the experimental measurements of CaO films has remained a

*Corresponding author: hannu.hakkinen@phys.jyu.fi

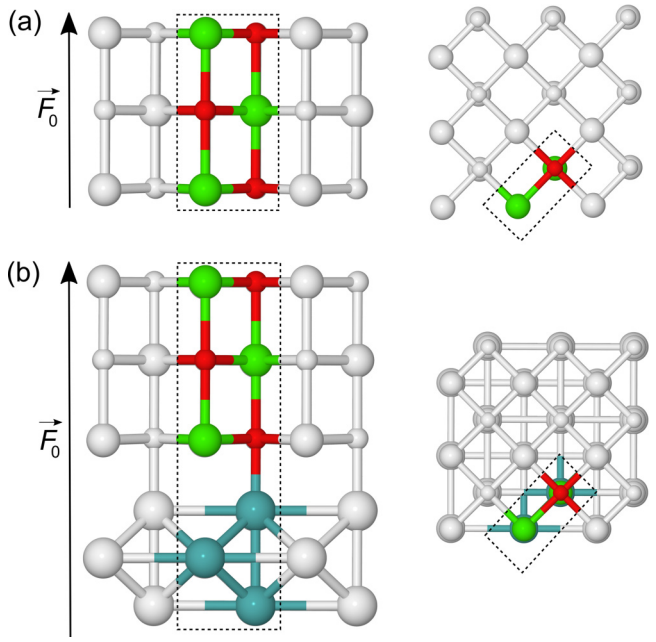

FIG. 1. Structural models of (a) 3-ML-thick unsupported CaO film and (b) 3-ML-thick CaO film supported by 3 ML Mo(100) used in the paper (green, Ca; red, O).

mystery. Nonetheless, the assumption about phonon-assisted transport through the CaO film can be carefully studied at the atomic scale by using a computational approach.

In this paper, we present a systematic study of a response of phonon frequencies and structural and electronic properties of CaO films with different thicknesses to the external static electric field. The use of the electric field enables reproduction of experimental sample bias in the STM setup. To assess an effect of a metallic substrate on the properties of oxide, freestanding and Mo(100) supported CaO films are investigated.

II. COMPUTATIONAL DETAILS

A. Electronic structure calculations

All calculations were performed using the CRYSTAL14 code within the framework of DFT [15]. The Perdew-Wang generalized gradient approximation exchange-correlation functional [16] with 10% of the Fock exchange part was utilized. The choice is due to the satisfied reproduction of experimental band gap for bulk CaO (∼7 eV is obtained by experiments [17,18], and the calculated value is 7.3 eV). A restricted set of calculations was performed using the classical Becke, three-parameter Lee-Yang-Parr (B3LYP) hybrid functional (20% of the Fock exchange) [19,20], but the results are similar and therefore will not be further discussed (some comparison can be found in Supplemental Material [21]). All-electron 8-411(d) [22] and 86-511(d21) basis sets were

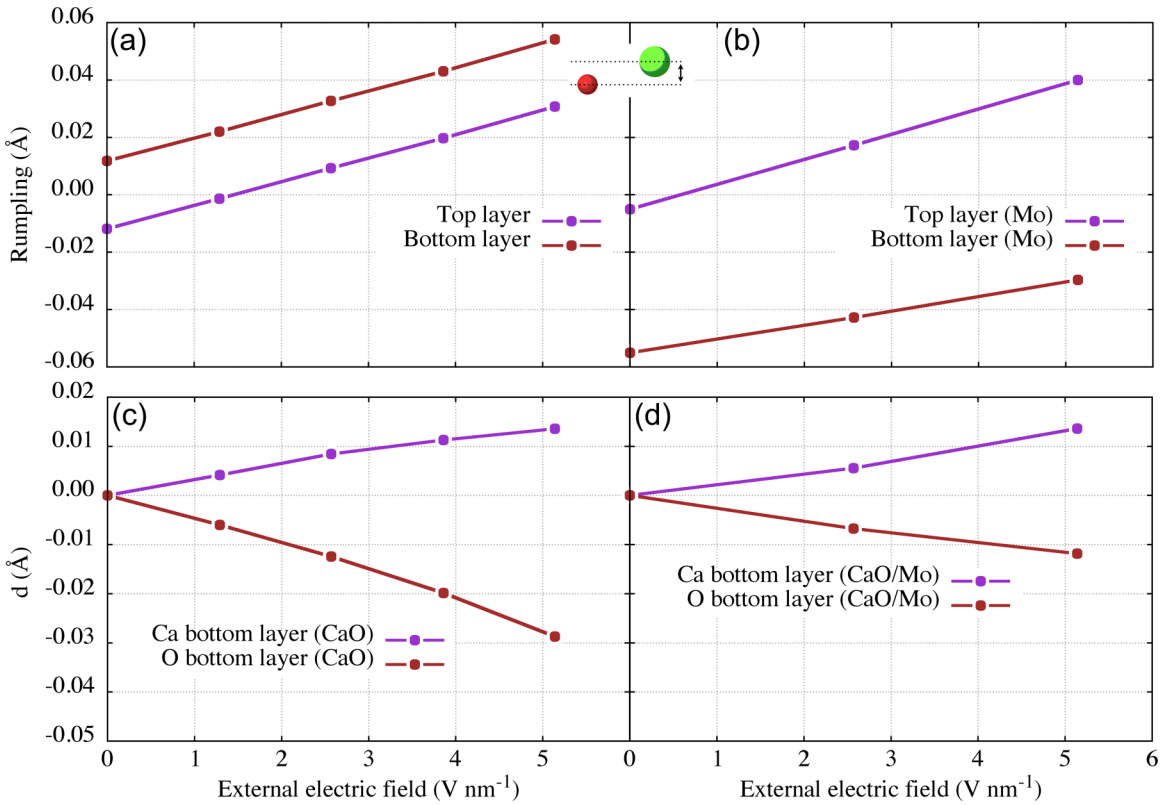

FIG. 2. Rumpling of relaxed z coordinates (in angstroms) of the top and bottom layers of (a) freestanding CaO and (b) CaO on Mo support films as a function of the external electric field and the effect of the external electric field on the relative positions of oxygen and calcium atoms in the top and bottom (c) freestanding CaO and (d) CaO layers on Mo support. Positions of oxygen and calcium atoms in the absence of the electric field are used as references in (c) and (d); i.e., $d(\text{ion}) = Z(\text{ion})_{x\,\text{V nm}-1} - Z(\text{ion})_{0\,\text{V nm}-1}$, where d is the change in the positions, Z is the absolute position of the corresponding ion, and x is the intensity of the external electric field.

used for O and Ca atoms, respectively. Such a combination of the DFT functional and basis sets reproduces the experimental lattice parameter for bulk CaO (4.81 Å experimental and 4.80 Å calculated) [23]. Effective core potential [24] was used to describe core electrons of the Mo atom, and the optimized def2-SV(P) [25] basis set was utilized for outer electrons (the optimized basis set is listed in Supplemental Material [21]). The reciprocal space for calculations of freestanding CaO films was sampled on a net of a 21 high-symmetry K points and for calculations of CaO/Mo(100) films was sampled on a 15 K points for a $1 \times 1 \times$ ML supercell. Tightened tolerance factors of 8, 8, 8, 8, and 16 were used for the evaluation of the Coulomb and exchange integrals. Geometry optimization for all structures was carried out using convergence criteria on total energy as $<10^{-7}$ arb. units ($<2.7 \times 10^{-6}$ eV) between Self-consistent field (SCF) cycles. Static electric field F_0 was applied along the nonperiodic z direction using the finite field perturbation method in terms of sawtooth bare potential [26], where F_0 values correspond to the displacement field with relation to the theoretical macroscopic field, $F : F = F_0/\varepsilon_0$, where ε_0 is the static dielectric constant. Calculations of phonons were carried out for optimized structures by using the $1 \times 1 \times$ ML and $3 \times 3 \times$ ML supercell approach. The irreducible Brillouin zone for the $3 \times 3 \times$ ML supercell contained three high-symmetry K points. More detailed computational details can be found in Supplemental Material [21].

B. Computational models of freestanding and Mo support CaO films

Calculations were carried out in a two-dimensional (x and y directions) periodic approach with a finite thickness along the z axis normal to the perfect (100) surface. Geometry optimization and calculations of phonon frequencies were implemented for CaO films in the absence and presence of an external static electric field applied along the nonperiodic z direction. The applied electric field lowers the symmetry of CaO films due to external perturbation and therefore makes the ions symmetrically inequivalent. Unsupported CaO films with the following thicknesses were investigated: 3, 5, 7, 9, 11, 13, and 15 ML. Lattice parameters and internal coordinates of freestanding CaO films were fully relaxed in the optimization procedure by using the respective symmetry group. Calculations of freestanding CaO films were repeated for the stepwise increased electric field ranging from 0.0025 to 0.01 arb. units in steps of 0.0025 arb. units that corresponds to 1.29, 2.57, 3.86, and 5.14 V nm^{-1}. Selection of the range of the external electric field values was motivated by typical experimental setups in STM papers [3]. Because the calculations with metallic support cause high computational demand, we limited the number of CaO films on Mo by exploring 3, 5, 7, and 11 ML. Internal coordinates were optimized for CaO/Mo(100) films, whereas the lattice parameter was kept fixed. The fixed lattice parameter was taken from the optimized structure of bulk Mo. Three Mo layers, where one from the bottom was frozen in the optimization of CaO/Mo(100) systems, were used as a support for CaO films. To examine the effect of the electric field on the properties and phonons of Mo supported CaO films, optimization and calculations of phonon frequencies were carried out at 2.57 and 5.14 V nm^{-1} of F_0. Figure 1 illustrates typical structural models used in the paper.

TABLE I. Distances between O and Mo atoms (in angstroms) calculated for CaO films with different thicknesses as a function of the external electric field.

F_0, V nm^{-1}	0	2.57	5.14
3 ML	2.269	2.259	2.254
5 ML	2.266	2.261	2.256
7 ML	2.268	2.262	2.255
11 ML	2.269	2.260	2.255

III. RESULTS AND DISCUSSION

A. Structural properties of freestanding and Mo supported CaO films

To check the response of structural properties of oxide films to the external static electric field, atomic shifts of Ca^{2+} and O^{2-} ions with respect to each other, so-called rumpling, in

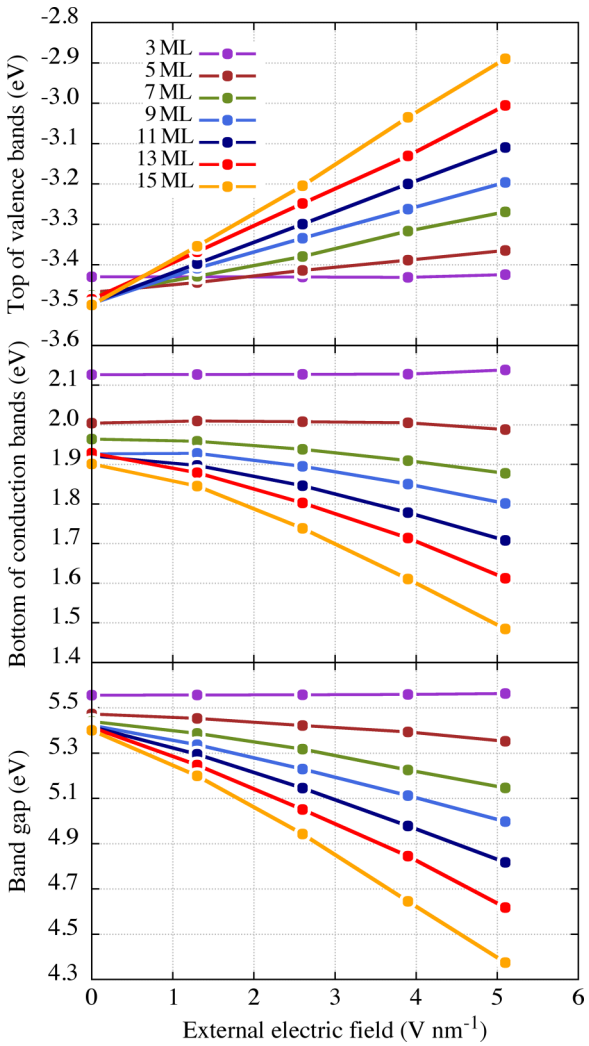

FIG. 3. Top of valence bands, bottom of conduction bands, and direct Γ-Γ band gaps for freestanding CaO films with different thicknesses calculated as a function of the external electric field. The top of the valence bands and the bottom of the conduction bands are reported with respect to the Fermi level.

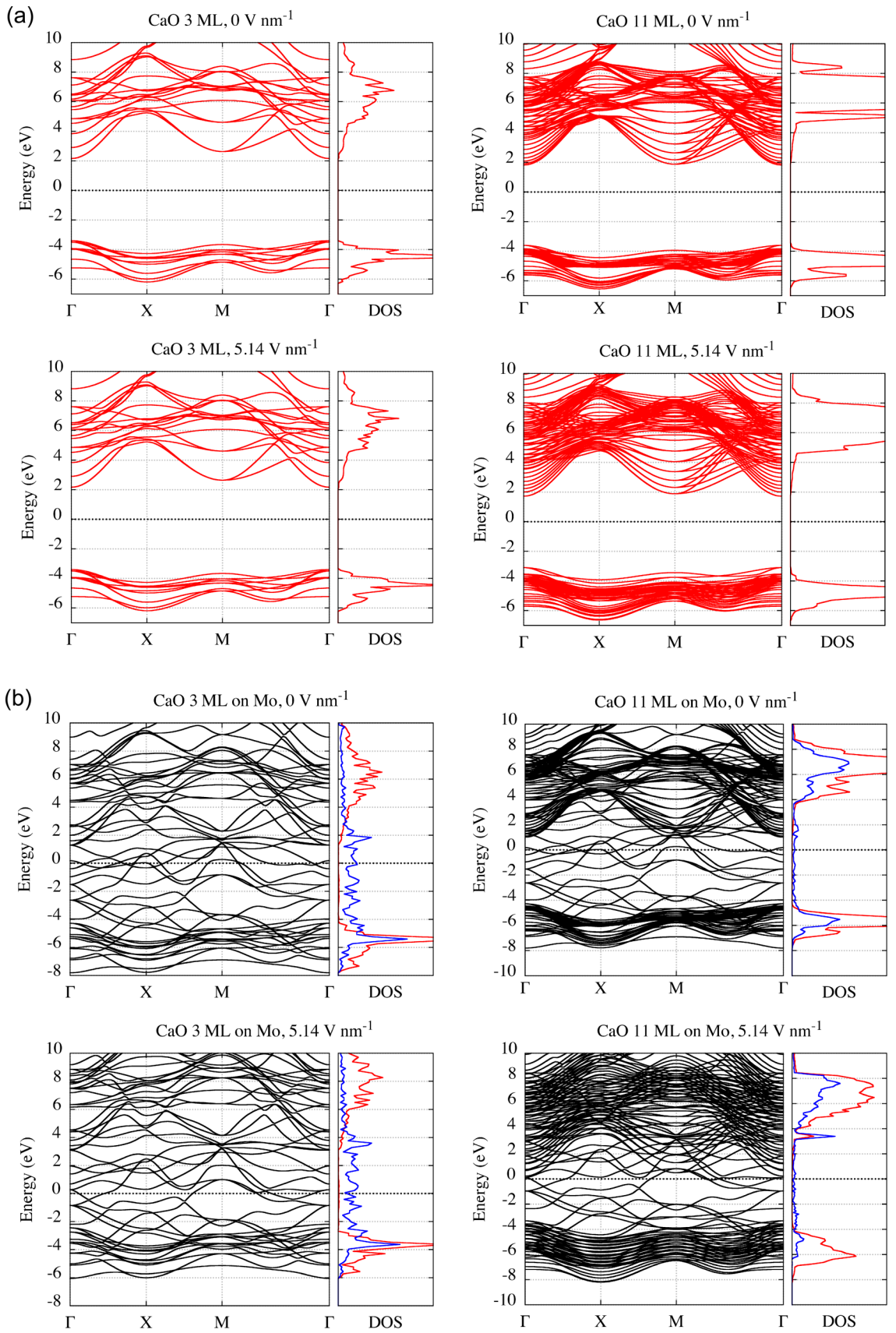

FIG. 4. Computed band structure and total DOS normalized to a CaO layer and a Mo atom, if applicable, of (a) freestanding and (b) supported by 3 ML Mo and 11 ML CaO films as a function of the external electric field (red lines, CaO; blue lines, Mo; black lines, CaO/Mo).

the topmost and bottom layers of CaO films were investigated [Figs. 2(a) and 2(b)]. Positive values mean that calcium ions are located higher than O^{2-} in the CaO layer.

We found that the rumpling of CaO layers is about the same within the considered range of the film thicknesses. Therefore, Figs. 2(a) and 2(b) depicts average rumpling among considered CaO films, depending on the applied electric field. The applied uniform electric field causes an internal relaxation of ions: an upward motion is detected for Ca^{2+} cations, whereas O^{2-} anions move downward according to the direction of the external electric field illustrated in Fig. 1. Thus, such expansion and contraction of the ions leads to complementary displacements. In general, the rumpling of CaO layers is negligible, with a maximum value of ~0.06 Å at 5.14 V nm^{-1} of the electric field. As expected, rumpling of the top layers of both freestanding and supported CaO films are about the same, whereas rumpling of the bottom layers becomes significantly smaller when the oxide is deposited on the Mo support. The bonding between bottom layer oxygen and molybdenum remarkably constrains movements of the O^{2-} ion, as seen in Figs. 2(c) and 2(d). Therefore, O^{2-}, being stacked by Mo support, is placed higher than calcium ions in the layer. At the same time, we see that the difference in the positions of Ca^{2+} atoms in freestanding CaO and CaO/Mo films is quite similar [Figs. 2(c) and 2(d)]. The rumpling of the middle CaO layers was analyzed, but we found it to be negligible due to stabilization of the adjacent layers. A response of lattice parameters of CaO films to the electric field was also investigated, but we find negligible effect within the considered range of F_0 values.

Table I summarizes interface distances between CaO films and Mo support. The distance between oxygen and molybdenum is constant with increasing film thickness. Our calculations show that the distances are shortened with the growing intensity of electric field, leading to ~0.01 Å decrease in the O-Mo bond length.

B. Electronic properties of freestanding and Mo supported CaO films

Next, we addressed the effect of the external static electric field on the electronic properties of CaO films. Figure 3 illustrates the calculated top of valence bands, bottom of conduction bands, and direct Γ-Γ band gaps of freestanding CaO films with different thicknesses as a function of external electric field.

We found that thickness of a CaO film has a minor effect on the electronic structure in the absence of the external electric field; small changes are detected, but they are almost negligible. Interesting features appear in the presence of the external electric field. Our results show that calculated direct Γ-Γ band gaps of CaO films are reduced with the increase of the electric field. In particular, the effect is found to be stronger for thicker CaO films so that 15 ML has the lowest band gap among the considered thicknesses. This effect is due to the widening of valence and conduction bands of oxide with growing intensity of the external electric field, as illustrated on 11 ML CaO film (Fig. 4).

As mentioned in Sec. II B, the applied electric field breaks the symmetry of oxide films and leads to the loss of degeneracy of energy levels. As a result, only ions from a given layer of CaO, i.e., the reference layer that is perpendicular to the field direction, remain equivalent. Therefore, polarization of the electron density associated with the reference layer of Ca^{2+} and O^{2-} ions to the adjacent oxide layers leads to an increase of band dispersion and, consequently, a reduction of the band gap. In other words, smearing of the density causes delocalization of the electronic states as seen, for example, in the extension of conduction and valence bands in density of states (DOS) plots of 11 ML CaO film under the applied electric field [Fig. 4(a)]. Likewise, we observe a negligibly small change in the electronic structure of 3 ML CaO in the presence of the electric field due to the minor band dispersion. A detailed explanation of these findings can be found in Refs. [27] and [28]. The electronic structure of CaO supported by Mo substrate systems is more sensitive to the applied electric field than are unsupported films. This finding is demonstrated by the greater extension of bands for 11 ML CaO/Mo film [Fig. 4(b)]. Furthermore, we found a new peak in the gap ~3 eV above the Fermi level in the presence of the external electric field. The electronic states of CaO and Mo seem to approach the same energy levels, which probably suggests that we observe the band bending effect. For 3 ML CaO/Mo, we have insignificant changes in DOS; however, the systematic shift of electronic bands is found in the presence of the external electric field.

C. Phonon frequencies of freestanding and Mo supported CaO films

Finally, the phonon modes were calculated at the Γ point. Similar to geometry optimization, calculations were carried out for freestanding and Mo supported CaO films in the selected values of the electric field as described in Sec. II B.

The $3N$-3 phonon modes of CaO films (N is the number of ions) can be classified according to their symmetry. For example, 3 ML CaO film has 15 internal degrees of freedom, giving rise to 10 normal modes; 5 in-plane modes belong to the E bidimensional representation and reflect transverse acoustic and optical phonons, and 5 out-of-plane modes belong to the A monodimensional representation and provide longitudinal acoustic and optical phonons.

Previous experimental and computational papers on CaO films demonstrate the correlation between the energy spacing of the dI/dV maxima and the highest energy longitudinal optical (heLO) phonon frequency calculated at the Γ point (Fig. 5) [14]. Herein, we examined phonon modes and

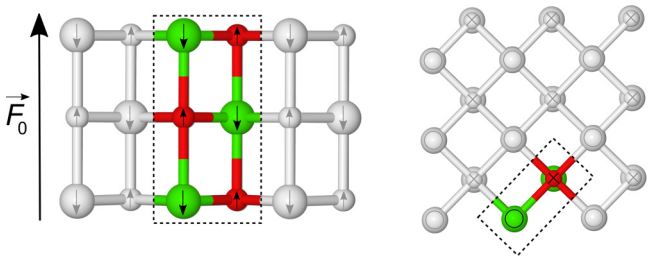

FIG. 5. Atomic displacements associated with the vertical interlayer normal mode that represents the Γ point LO phonon of 3 ML CaO film (green, Ca; red, O; turquoise, Mo).

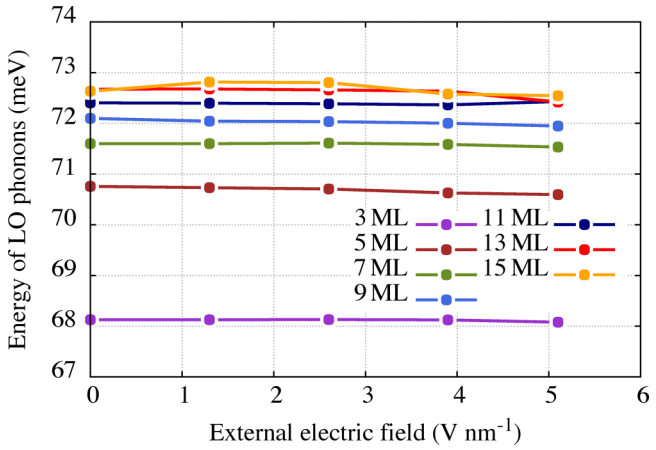

FIG. 6. The calculated energies of the Γ point heLO phonon of CaO films with different thicknesses as a function of the external electric field.

their respective energies and found that the highest energy mode for all considered CaO films corresponds to the same heLO phonon (Fig. 5). A few examples showing all phonon frequencies are presented in Supplemental Material [21], and the following discussion focuses on the heLO phonon of the freestanding and Mo supported CaO films.

Figure 6 summarizes calculated energies of the heLO phonon as a function of film thickness and external electric field. In line with experimental findings, we observe the gradual increase of the energy of the heLO phonon as a function of film thickness [14]. With increasing film thickness, the frequency of the heLO phonon approaches the value computed for bulk CaO: we obtained 72.7 meV for 11 ML, 73.3 meV for 21 ML, and 73.9 meV for the bulk with the B3LYP functional. The LO phonon from CaO powder spectra was measured to be 71.30 meV [29], and similar values are obtained from neutron spectroscopy [30]. DFT calculations for bulk CaO employing the local density approximation (LDA) functional give an LO phonon frequency of 70.6 meV calculated at the Γ point [31]; the value is slightly smaller that corresponding to experimental energy. In Fig. 6, we see a significant energy shift from ultrathin 3 ML CaO to thicker films. The difference in energies for films with a thickness higher than 3 ML is typically small. It can be explained by thick CaO films tending to have more vivid bulk behavior, while the ultrathin 3 ML CaO film undergoes reconstruction to minimize the energy. Moreover, it is evident that influence of the external electric field on phonons is negligible and this is true for other phonon modes (see Supplemental Material [21]). For comparison, the effect of the electric field on the phonons of a softer material, namely, NaCl, was addressed at the B3LYP level of theory (see Supplemental Material [21]). However, an

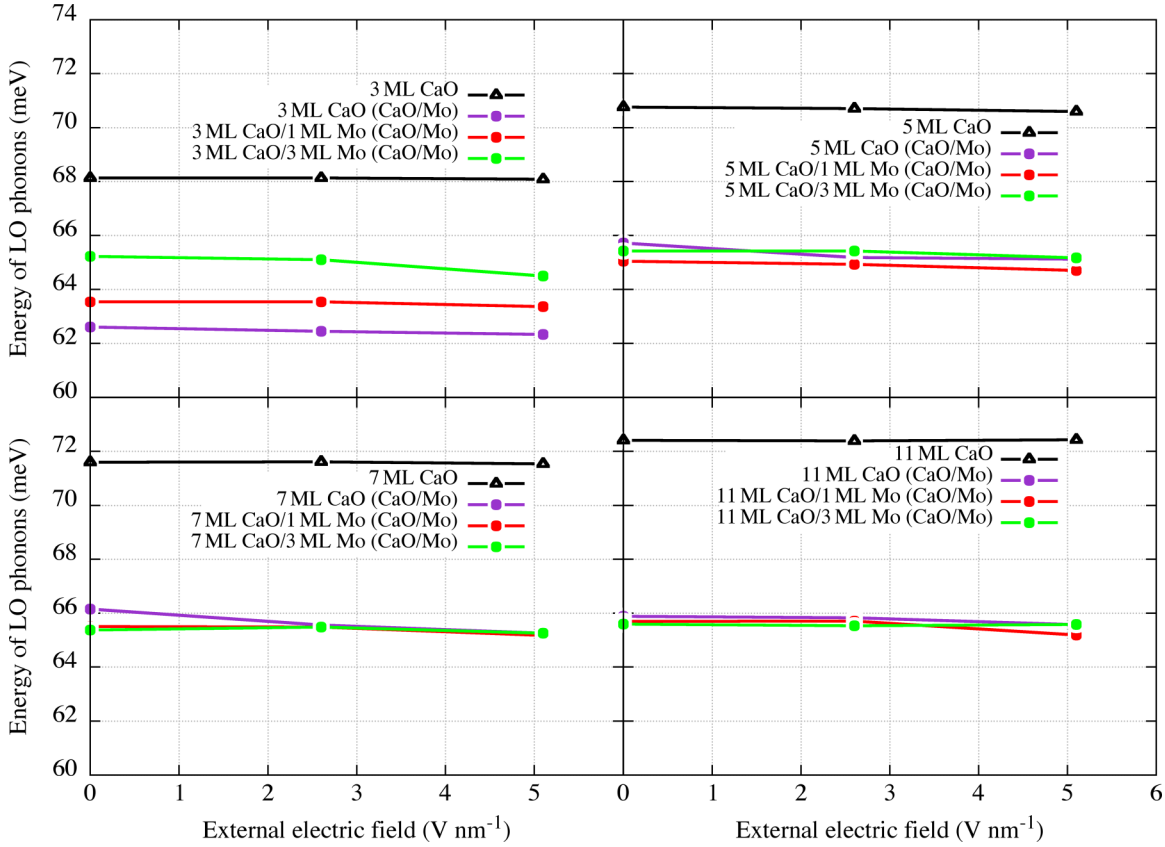

FIG. 7. Calculated energies of the Γ point LO phonons of CaO and CaO/Mo films with different thicknesses as a function of the external electric field by using different structural models (black lines, optimized unsupported films; purple lines, optimized on 3 ML Mo(100) supported films and phonons calculated for CaO films with all Mo layers discarded; red lines, optimized on 3 ML Mo(100) supported films and phonons calculated for CaO films with two bottom Mo layers discarded; green lines, optimized on 3 ML Mo(100) supported films and phonons calculated for the complete system).

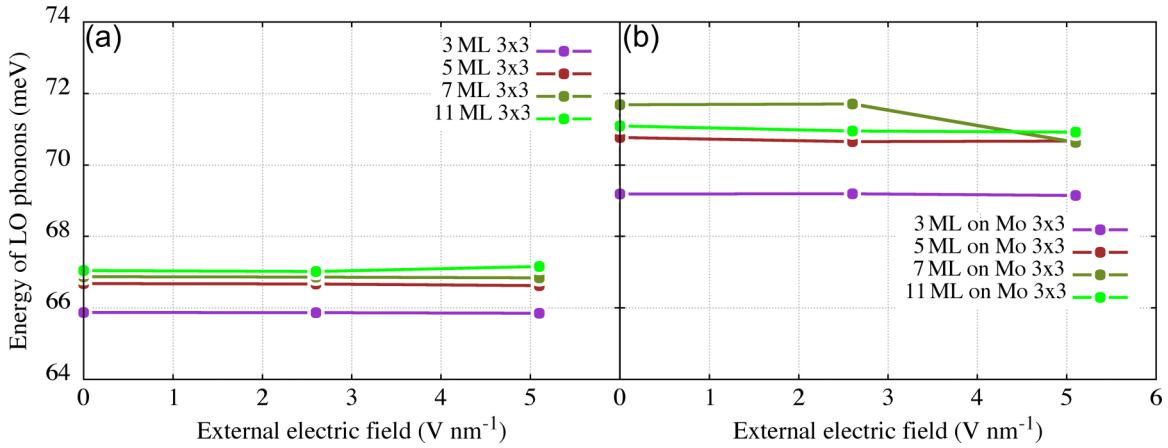

FIG. 8. Calculated average energies of heLO phonons for (a) freestanding and (b) Mo supported CaO films with different thicknesses as a function of the external electric field using a 3 × 3 supercell.

insignificant effect of the electric field was observed in this case as well.

Next, we investigated the effect of the Mo substrate on the phonon frequencies of the CaO films (Fig. 7). To our knowledge, this is the first paper in which phonons of metal supported CaO films are calculated under the applied external electric field. Therefore, to address the role of Mo support, three structural models were adopted for calculations of phonons: (1) complete CaO/Mo(100) systems, (2) CaO/Mo(100) systems with two bottom Mo layers discarded, and (3) CaO/Mo(100) systems with all molybdenum layers discarded.

First, we found that the highest energy phonon mode for CaO/Mo films is identical to the heLO phonon illustrated in Fig. 5. Our results demonstrate that the heLO phonon frequency obtained for films supported by Mo is typically independent of the chosen structural model for the calculations under the applied external electric field, and it gives ∼66 meV. Similar to freestanding CaO films, we found gradual growth of the energies of the heLO phonons of Mo supported CaO films as a function of the electric field; however, the increase is even smaller in this case. We observe that difference in the energies of heLO phonons calculated for the three structural models becomes negligible with the thickness of oxide. This finding can be explained by how, in the presence of Mo support, thinner films lose a larger fraction of the degrees of freedom compared to thicker films; therefore, Mo support has a smaller impact on phonon frequencies of thicker CaO, and vice versa. Furthermore, we found that geometry optimization of CaO films on Mo support is important for phonon calculations of thicker films. In particular, the highest difference in the energies of the heLO phonon is observed between optimized freestanding 11 ML CaO films (black line in Fig. 7) and Mo supported CaO films (purple, red, and green lines in Fig. 7).

Finally, we explored phonon dispersion of freestanding and Mo supported CaO films by using a 3 × 3 supercell (see Sec. II) for 3, 5, 7, and 11 ML as a function of the external electric field with given values of 2.57 and 5.14 V nm^{-1} to compare the results for phonons calculated at the Γ point only (Fig. 8). Because calculations of phonon dispersion are highly demanding, frequencies for optimized CaO films on Mo support were computed only for Ca and O atoms as in structural model 3, described above.

Each point on the plot reflects the average value of the energy of heLO phonon for the CaO film calculated in different **q** vectors using the supercell approach. Overall, this approach provides three unique values for each phonon mode of CaO films. Here, we also noticed the gradual increase of the energy of the heLO phonon as a function of film thickness. The exception, though, is seen for the CaO 11 ML/Mo system in the absence and at the given 2.57 V nm^{-1} intensity of the electric field compared with 7 ML, but under 5.14 V nm^{-1} of F_0 11 ML, CaO reflects the highest heLO energy again. In general, phonon frequencies calculated for CaO/Mo systems seem to be systematically higher in energy than for unsupported films, but the only negligible effect of the external electric was found for both systems in this case.

Table II represents the effect of the supercell approach on the heLO phonons for CaO films by giving the standard deviation between calculated values. Three values of the energy of heLO phonons were obtained for each phonon mode. Therefore, these data can be interpreted as the deviation from the average value of the heLO phonons of CaO films. For example, the energy of the heLO phonon of the CaO 11 ML/Mo system is possibly varied from ∼70 to ∼80 V nm^{-1}. The standard deviation was found to be larger for supported CaO films than for freestanding ones, highlighting the importance of the supercell approach for these systems.

TABLE II. Standard deviation of calculated heLO phonon energies in different **q** vectors of CaO and CaO/Mo films as a function of the external electric field.

F_0, V nm^{-1}	0	2.57	5.14
3 ML	5.76	5.75	5.73
5 ML	6.28	6.26	6.23
7 ML	6.55	6.55	6.52
11 ML	6.86	6.87	7.09
3 ML Mo	8.70	8.79	8.83
5 ML Mo	8.41	8.40	8.59
7 ML Mo	7.51	7.56	8.14
11 ML Mo	8.20	8.15	8.31

IV. CONCLUSION

We performed systematic DFT computational study on the properties and phonon frequencies of CaO films with different thicknesses as a function of the external static electric field. To assess the effect of a metal support, freestanding and Mo(100) supported CaO films were investigated. We found that the response of structural properties of CaO films to the applied electric field is negligible regarding ionic relaxation. However, the influence of the electric field was shown to be significant on the electronic structure of CaO, leading to the reduction of direct Γ-Γ band gaps with a more pronounced effect for the thicker oxide films. It is explained by band dispersion due to the polarization of the electron density of a given layer of ions to adjacent layers in the film. Furthermore, we demonstrated that effect of the external electric field is even stronger for Mo supported CaO films. Phonons of CaO films were shown to be negligibly affected by the applied static electric field. The slight gradual increase of the energy of phonons as a function of CaO film thickness was found to be in line with earlier experimental findings. Herein, Mo support seems to have a larger effect on thicker oxide films by decreasing energy of the phonon modes comparing to the freestanding CaO.

ACKNOWLEDGMENTS

This paper was financially supported by the Academy of Finland (Project No. 294217 and Academy professorship to H.H.). Computer resources from the Finnish IT Center for Science are gratefully acknowledged. A.S.B. and K.H. acknowledge financial support from the Academy of Finland (Grant No. 277222). S.T. acknowledges the support of the Cineca computing center through an Italian SuperComputing Resource Allocation (ISCRA) project (Project ID HP10BD69EF). We thank N. Nilius, H. J. Freund, and W. D. Schneider for useful discussions.

[1] G. Pacchioni and H. Freund, Chem. Rev. **113**, 4035 (2013).
[2] H. Freund and G. Pacchioni, Chem. Soc. Rev. **37**, 2224 (2008).
[3] N. Nilius, Surf. Sci. Rep. **64**, 595 (2009).
[4] L. Giordano and G. Pacchioni, Acc. Chem. Res. **44**, 1244 (2011).
[5] K. Honkala, Surf. Sci. Rep. **69**, 366 (2014).
[6] M. Sterrer, T. Risse, U. M. Pozzoni, L. Giordano, M. Heyde, H. P. Rust, G. Pacchioni, and H.-J. Freund, Phys. Rev. Lett. **98**, 096107 (2007).
[7] M. Muntwiler and X. Y. Zhu, Phys. Rev. Lett. **98**, 246801 (2007).
[8] C. Kittel, *Introduction to Solid State Physics*, 6th ed. (John Wiley & Sons, New York, 1986).
[9] G. P. Srivastava, *The Physics of Phonons* (Hilger, Bristol, 1990).
[10] J. Repp, G. Meyer, S. Paavilainen, F. E. Olsson, and M. Persson, Phys. Rev. Lett. **95**, 225503 (2005).
[11] H. Zheng, J. Kröger, and R. Berndt, Phys. Rev. Lett. **108**, 076801 (2012).
[12] N. Spiridis, M. Zajac, P. Piekarz, A. I. Chumakov, K. Freindl, J. Goniakowski, A. Kozioł-Rachwał, K. Parlinski, M. Ślęzak, T. Ślęzak, U. D. Wdowik, D. Wilgocka-Ślęzak, and J. Korecki, Phys. Rev. Lett. **115**, 186102 (2015).
[13] X. Shao, P. Myrach, N. Nilius, and H.-J. Freund, J. Phys. Chem. C **115**, 8784 (2011).
[14] Y. Cui, S. Tosoni, W.-D. Schneider, G. Pacchioni, N. Nilius, and H.-J. Freund, Phys. Rev. Lett. **114**, 016804 (2015).
[15] R. Dovesi, V. R. Saunders, C. Roetti, R. Orlando, C. M. Zicovich-Wilson, F. Pascale, B. Civalleri, K. Doll, N. M. Harrison, I. J. Bush, Ph. D'Arco, M. Llunell, M. Causa, and Y. Noel, *CRYSTAL14 User's Manual* (University of Torino, Torino, Italy, 2016).
[16] J. P. Perdew, J. A. Chevary, S. H. Vosko, K. A. Jackson, M. R. Pederson, D. J. Singh, and C. Fiolhais, Phys. Rev. B **46**, 6671 (1992).
[17] R. C. Whited and W. C. Walker, Phys. Rev. **188**, 1380 (1969).
[18] R. C. Whited, C. J. Flaten, and W. C. Walker, Solid State Commun. **13**, 1903 (1973).
[19] A. D. Becke, J. Chem. Phys. **98**, 5648 (1993).
[20] P. J. Stephens, F. J. Devlin, C. F. Chabalowski, and M. J. Frisch, J. Phys. Chem. **98**, 11623 (1992).
[21] See Supplemental Material at http://link.aps.org/supplemental/10.1103/PhysRevB.95.165423 for the comparison of the results obtained by different functionals and additional computational details.
[22] L. Valenzano, F. J. Torres, K. Doll, F. Pascale, C. M. Zicovich-Wilson, and R. Dovesi, Z. Phys. Chem. **220**, 893 (2006).
[23] P. Pichet, H. K. Mao, and P. M. Bell, J. Geophys. Res. **93**, 15279 (1988).
[24] D. Andrae, U. Haeussermann, M. Dolg, H. Stoll, and H. Preuss, Theor. Chim. Acta **77**, 123 (1990).
[25] F. Weigend and R. Ahlrichs, Phys. Chem. Chem. Phys. **7**, 3297 (2005).
[26] C. Darrigan, M. Rerat, G. Mallia, and R. Dovesi, J. Comput. Chem. **24**, 1305 (2003).
[27] C. S. Praveen, A. Kokalj, and M. Valant, Comp. Mater. Sci. **50**, 2628 (2011).
[28] C. S. Praveen, A. Kokalj, M. Rerat, and M. Valant, Solid State Sci. **14**, 1412 (2012).
[29] M. Galtier, A. Montaner, and G. Vidal, J. Phys. Chem. Solid **33**, 2295 (1972).
[30] D. H. Saunderson and G. E. Peckham, J. Phys. C **4**, 2009 (1971).
[31] O. Schütt, P. Pavone, W. Windl, K. Karch, and D. Strauch, Phys. Rev. B **50**, 3746 (1994).